International Journal on Magnetic Particle Imaging
Vol 9, No 1, Suppl 1, Article ID 2303022, 4 Pages

Infinite Science Publishing

Proceedings Article

Using Negative Bolus in Dynamic MPI

Fabian Mohn [a,b,*] · Miriam Exner [a,b] · Patryk Szwargulski [a,b] · Martin Möddel [a,b] · Tobias Knopp [a,b] · Matthias Graeser [c,d]

[a] Section for Biomedical Imaging, University Medical Center Hamburg-Eppendorf, Hamburg, Germany
[b] Institute for Biomedical Imaging, Hamburg University of Technology, Hamburg, Germany
[c] Fraunhofer Research Institute for Individualized and Cell-based Medicine, IMTE, Lübeck, Germany
[d] Institute for Medical Engineering, University of Lübeck, Lübeck, Germany
[*] Corresponding author, email: fabian.mohn@tuhh.de

Abstract

In Magnetic Particle Imaging, the spatial distribution of a tracer is measured and depicted with a concentration dependent signal intensity for any location that contains particles, whereas surrounding tissue does not provide any signal. After tracer injection, the signal over time (positive contrast) can be utilized as a transient response to calculate dynamic diagnostic parameters like perfusion parameter maps. In this work, a bolus of physiological saline solution without any particles (negative contrast) is proposed, where the remaining steady state concentration contributes to the image contrast. This opens up the possibility to stretch the total monitoring time of a patient by utilizing a positive-negative contrast sequence, while keeping the total iron dose constant in the subject. Resulting time responses show that normalized signals from positive and negative boli are concurrent in the phantom experiments, indicating identical diagnostic parameters for *in-vivo* use.

I. Introduction

In Magnetic Particle Imaging (MPI), the visualization of tracer is based on its exposure to a range of different magnetic fields for excitation and spatial selection [1]. Image reconstruction in MPI yields a snapshot of the spatial tracer distribution. In other words, an image signal greater than zero will be reconstructed where particles are located (positive contrast). Vice versa, regions without tracer do not contribute signal to the image. In Magnetic Resonance Imaging (MRI), which is a tracer-free imaging modality, the hydrogen distribution is imaged [2]. However, for specific types of imaging, contrast agents are used to decrease the signal intensity of T_2^*-weighted images by locally accelerating the dephasing of magnetization, hence a signal reduction is created [3, 4]

Independent of the modality, the underlying principle for dynamic imaging is the same: to trace the shape of the peak in signal increase or reduction over time and location, so diagnostic parameters e.g. for perfusion imaging can be calculated [5, 6]. In MPI, this approach has been successfully used for perfusion imaging in acute stroke [7] and pulmonary blood volume estimation [8]. Both works used tracer boli to create a positive contrast.

In future clinical applications of MPI, however, if a monitoring of a stroke patient is planned, a regular dose has to be administered, which can lead to significant accumulation of the tracer. To minimize the overall amount of tracer and to heed limitations of the total injectable iron mass of a patient (in concentration and/or for a certain period of time), we suggest the application of negative boli. Negative boli do not contain tracer and cause a reduction of the measured signal intensity of MPI signals, which is then utilized to calculate diagnostic parameters. The underlying principle requires a minimum baseline or steady-state concentration of tracer to be present, so

a negative bolus consisting of saline solution leads to signal reduction of the baseline signal. A possible approach is to switch from positive to negative boli, as soon as a sufficient image signal-to-noise ratio (SNR) is reached by the steady state concentration.

In this work, we show that signals from positive and negative boli are concurrent and deviations in shape are low after normalization. Our study employs a circulatory experimental setup with a a rat-scaled heart phantom on a pre-clinical MPI system.

II. Methods and materials

The proposed method in this paper requires a baseline tracer concentration, that could be reached with a single large initial bolus or accumulated over time by several smaller positive boli. Once the tracer concentration has reached a homogeneous steady-state, a bolus of neutral saline solution can be imaged due to the negative contrast (a minimum in signal intensity) that is created by tracer displacement and perfusion parameters can be derived. Positive boli serve as a ground truth in this work and verification is done by comparing dynamic images and normalized time curves between both positive and negative bolus types.

Experimental Setup. The setup consists of a peristaltic pump that circulates the imitated blood pool (desalinated water) at a realistic cardiac output for a rat (31 ml/ min). As shown in Figure 1 (a), the fluid passes a reservoir (syringe) of 1 ml first, which acts as a pressure compensation when a bolus is injected that increases the total volume in the imitated blood pool. A 3D printed trap for air bubbles follows, which filters arising air from pressure variation or by injection to prevent trapped air in the phantom. Next comes the injection point at a realistic distance (caudal vein) from the heart phantom, followed by the heart phantom [9] itself which is located inside the scanner bore. The total volume of the imitated blood pool is similar to the blood volume of a rat (14 ml). The heart phantom is a flow phantom that consists out of 4 chambers (left/right atrium/ventricle) and was placed in the center of the field of view (FOV) via a robotic mount.

Experiments. A baseline concentration of 237 μg_{Fe}/ml perimag (micromod GmbH, Rostock, Germany) was chosen as initial bolus. Then, alternating positive and negative boli were applied and the time response throughout different regions of the heart phantom was recorded. Boli of 150 µL were chosen, either as a tracer dispersion of 1 mg_{Fe}/ml (positive) or consisting of neutral saline solution (negative). During bolus injection, the pump kept circulating the imitated blood pool and the scanner was running a measurement for 4 minutes continuously until the bolus was homogeneously distributed.

Reconstruction. Images were reconstructed using the system matrix approach implemented by a Kaczmarz-solver with a penalizing regulation parameter $\lambda = 0.1$, an SNR-threshold of 5 for frequency selection and 5 iterations [10]. The raw data is processed according to Figure 1 (b) to yield filtered data. Plots in Figure 3 (b) include an additional normalization step via linear regression to match maxima without distorting the underlying time axis. In this way, the shapes of positive and negative boli can be overlaid e.g. to compare rise times or the area under the curve (AUC). Normalized data was also Hann-filtered in Figure 3 (b). 2D subtractions images use the filtered data and are calculated by subtracting the concentration distribution just prior to bolus injection from all depicted frames. Time curves of specific positions are tracked by selecting a single voxel, since the phantom is static during measurements.

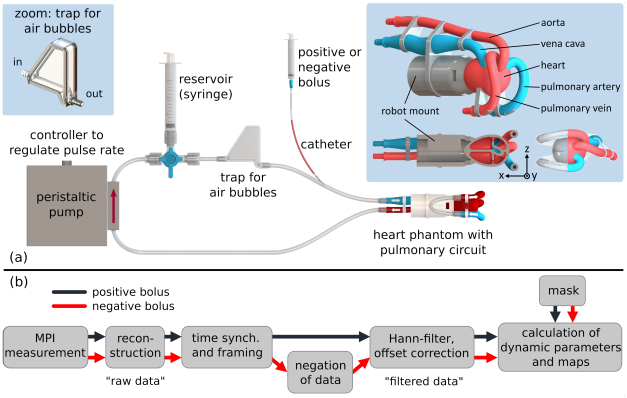

Figure 1: Rat-scale experimental setup. Following parts constitute the experimental setup (a), stated in flow direction: peristaltic pump, reservoir (syringe), trap for air bubbles, injection at vena caudalis, 3D printed heart phantom, return tube. Pump, reservoir and air trap are located outside the scanner. Below in (b), the data processing flow chart is depicted. The relevant time frame is selected from reconstructed data, negated for negative boli, and filtered for further processing.

Hardware. The pre-clinical MPI scanner (Bruker, Ettlingen, Germany) was operated with drive field strengths of 12 mT in all three spatial dimensions and a gradient field strength of 1.2 T m^{-1} in z-direction that result in a FOV of 40 × 40 × 20 mm^3. The acquisition speed was 21.54 ms per frame and a custom receive chain with a gradiometric receive coil insert (bore diameter 72 mm) was used, similar to the insert in [11].

III. Results

A single positive bolus (filtered data) is displayed in Figure 2 (a) for different positions in the heart phantom with the respective dynamic time curves. This visualizes the delay (transition times between different areas) and the shape as the sharp peak of the bolus disperses with time. Subtraction images are shown below in (b), indicating

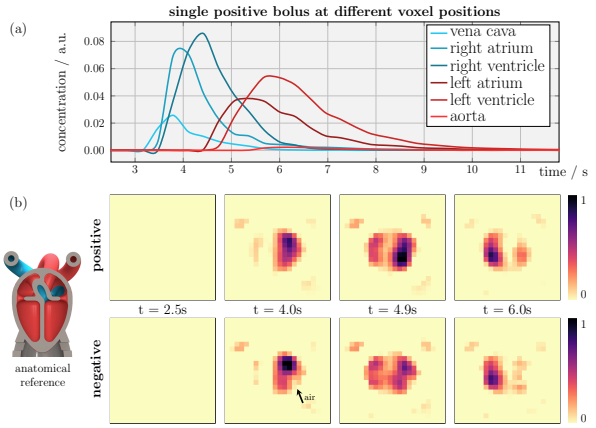

Figure 2: Dynamic images. In (a), different voxels in the heart phantom are tracked to observe the time response of a single bolus at various locations (filtered data). Below in (b), subtraction images are shown for a positive and a negative bolus with the anatomical reference slice on the left (processed as depicted in Figure 1 (b)). Despite all efforts to avoid air pockets, a small bubble got trapped.

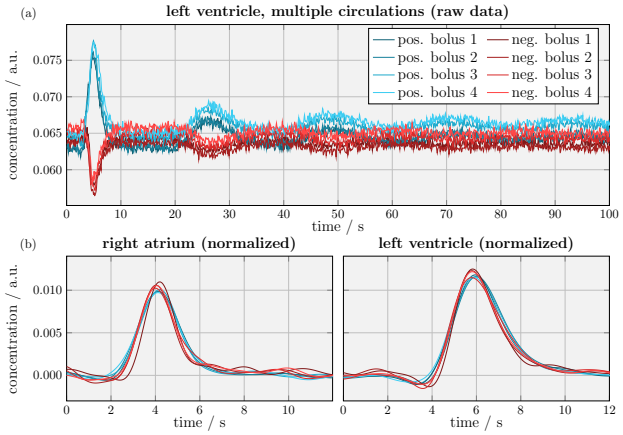

Figure 3: Raw data and normalized results. On the top, the raw data of 8 boli is shown for 100 s and several bolus passings are visible. The bottom shows the right atrium (highest deviations) and the left ventricle (best case) after Hann-filtering and normalization.

that they can successfully be calculated for negative boli and they show no significant deviations from the positive ground truth. The bolus can be seen to enter the right ventricle first, then passing on to the left side of the heart.

Figure 3 shows the time response of 4 positive and 4 negative boli, without normalization in (a), but all offsets were corrected to start at zero. Over 100 seconds, several passings of both, the positive and the negative boli, through the left ventricle are observable and their respective steady-state concentrations become visible. Peaks of negative boli are about 43% lower in the raw data. On the bottom in (b), the normalized curves of all 8 boli are shown for the right atrium and the left ventricle. Negative rise times are on average shorter, or in other words the full width at half maximum (FWHM) is smaller, although the normalized data shows no significant deviations for all samples. The shape of the curvature and the AUC are almost identical.

IV. Discussion and conclusion

As shown in Figure 3, the normalization of positive and negative boli was successful in phantom experiments. The difference in extrema in the raw data depends on the chosen baseline concentration and on the positive bolus concentration, both of which can be chosen differently. Although rise times and the FWHM are on average shorter for negative boli, the visible deviation is small in Figure 3 (b). A systematical fault in the setup is unlikely, because boli were applied with identical procedure and alternatingly. In Figure 2 (a), some deviations from expectations are visible, e.g. the bolus in the vena cava should be the highest with the lowest FWHM and all boli should roughly have the same AUC. Limited resolution and unfortunate voxel-spacing may cause small vessels of the phantom to contain some phantom border (partial volume effect). Similar to other imaging modalities, resolution and motion artifacts will be challenging for future *in-vivo* imaging, which require more sophisticated voxel tracking techniques than selecting a single static voxel. However, the different regions of the heart can clearly be identified during both bolus transitions in Figure 2 (b).

Although all negative boli could be normalized, the amount of 8 total injections does not yield statistical reliability and further investigation of different concentrations and volumes should be conducted. The boli need to be of identical volume for a successful normalization, which was confirmed in other experiments. Regarding the choice of a baseline concentration that is indulgent for the patient, positive boli should be chosen as small as imaging allows. Multiple positive boli can be applied until a sufficient image SNR of the blood pool is reached (steady-state) and negative boli become feasible, before safety limits of maximum iron amounts are exhausted. Now, negative boli allow to continue to calculate dynamic diagnostic parameters, without adding to the total iron amount in the body. The maximum achievable SNR for a negative bolus is limited by the image SNR in advance to the injection. A complete washout of all particles in a volume of interest by a large negative bolus would cause maximum SNR for the negative bolus. However, this results in an intensity plateau and is undesirable, just as clipping of a positive bolus is, and makes the correct calculation of perfusion parameters more difficult. A combination of positive-negative injections will enable a longer observation time of a patient, where negative boli provide extra imaging without adding to the iron concentration.

10.18416/ijmpi.2023.2303022

Author's statement

Conflict of interest: Authors state no conflict of interest.

References

[1] B. Gleich and J. Weizenecker. Tomographic imaging using the nonlinear response of magnetic particles. *Nature*, 435(7046):1214–1217, 2005, doi:10.1038/nature03808.

[2] P. C. Lauterbur. Image Formation by Induced Local Interactions: Examples Employing Nuclear Magnetic Resonance. *Nature*, 242(5394):190–191, 1973, doi:10.1038/242190a0.

[3] E. L. Barbier, L. Lamalle, and M. Décorps. Methodology of brain perfusion imaging: Methodology of Brain Perfusion Imaging. *Journal of Magnetic Resonance Imaging*, 13(4):496–520, 2001, doi:10.1002/jmri.1073.

[4] P. Keston, A. D. Murray, and A. Jackson. Cerebral Perfusion Imaging using Contrast-enhanced MRI. *Clinical Radiology*, 58(7):505–513, 2003, doi:10.1016/S0009-9260(03)00130-2.

[5] D. S. Williams, J. A. Detre, J. S. Leigh, and A. P. Koretsky. Magnetic resonance imaging of perfusion using spin inversion of arterial water. *Proceedings of the National Academy of Sciences*, 89(1):212–216, 1992, doi:10.1073/pnas.89.1.212.

[6] J. A. Detre, J. S. Leigh, D. S. Williams, and A. P. Koretsky. Perfusion imaging. *Magnetic Resonance in Medicine*, 23(1):37–45, 1992, doi:10.1002/mrm.1910230106.

[7] P. Ludewig, N. Gdaniec, J. Sedlacik, N. D. Forkert, P. Szwargulski, M. Graeser, G. Adam, M. G. Kaul, K. M. Krishnan, R. M. Ferguson, A. P. Khandhar, P. Walczak, J. Fiehler, G. Thomalla, C. Gerloff, T. Knopp, and T. Magnus. Magnetic Particle Imaging for Real-Time Perfusion Imaging in Acute Stroke. *ACS Nano*, 11(10):10480–10488, 2017, doi:10.1021/acsnano.7b05784.

[8] M. G. Kaul, T. Mummert, M. Graeser, J. Salamon, C. Jung, E. Tahir, H. Ittrich, G. Adam, and K. Peldschus. Pulmonary blood volume estimation in mice by magnetic particle imaging and magnetic resonance imaging. *Scientific Reports*, 11(1):4848, 2021, doi:10.1038/s41598-021-84276-9.

[9] M. Exner, P. Szwargulski, T. Knopp, M. Graeser, and P. Ludewig. 3D Printed anatomical model of a rat for medical imaging. *Current Directions in Biomedical Engineering*, 5(1):187–190, 2019, Place: Berlin, Boston Publisher: De Gruyter. doi:10.1515/cdbme-2019-0048.

[10] T. Knopp, P. Szwargulski, F. Griese, M. Grosser, M. Boberg, and M. Möddel. MPIReco.jl: Julia package for image reconstruction in MPI. *International Journal on Magnetic Particle Imaging*, 5(1), 2019, doi:10.18416/ijmpi.2019.1907001.

[11] M. Graeser, T. Knopp, P. Szwargulski, T. Friedrich, A. Von Gladiss, M. Kaul, K. M. Krishnan, H. Ittrich, G. Adam, and T. M. Buzug. Towards Picogram Detection of Superparamagnetic Iron-Oxide Particles Using a Gradiometric Receive Coil. *Scientific Reports*, 7(1):6872, 2017, doi:10.1038/s41598-017-06992-5.